Available online at www.sciencedirect.com
SCIENCE DIRECT
Solid State Communications 132 (2004) 1–5
solid state communications
www.elsevier.com/locate/ssc

Efficient free exciton emission at room temperature in $Zn_{0.5}Cd_{0.5}Se/Mg_xZn_yCd_{1-x-y}Se$ quantum wells

O. Maksimov[a,*], N. Samarth[a], H. Lu[b], Martin Muñoz[c], M.C. Tamargo[b]

[a]Department of Physics, Pennsylvania State University, 104 Davey Lab, University Park, PA 16802, USA
[b]Department of Chemistry, City College of New York, New York, NY 10031, USA
[c]Department of Physics, Virginia Commonwealth University, Richmond, VA 23284, USA

Received 17 June 2004; received in revised form 7 July 2004; accepted 12 July 2004 by E.L. Ivchenko
Available online 28 July 2004

Abstract

We use temperature and power-dependent photoluminescence spectroscopy to demonstrate efficient free exciton emission at room temperature in high quality, strongly confining $Zn_{0.5}Cd_{0.5}Se/Mg_xZn_yCd_{1-x-y}Se$ quantum wells. Our measurements indicate that at low temperatures ($T<50$ K), the luminescence is dominated by bound exciton emission. However, free exciton emission becomes dominant at high temperatures ($T>100$ K) and persists up to room temperature with an intensity that is ~40% that at cryogenic temperatures. We attribute these observations to the deep confinement potential that stabilizes excitons and prevents their thermal escape.

PACS: 71.35.Cc; 71.55.Gs; 78.55.Et

Keywords: A. ZnCdSe; B. Molecular beam epitaxy; E. Photoluminescence

Although substantial success has been achieved in the development of $Al_xIn_yGa_{1-x-y}N$-based blue laser diodes (LDs), it is more challenging to produce long-lived devices operating in the green-yellow region (530–590 nm) due to the high threshold current density required for lasing [1]. Since $Al_xGa_yIn_{1-x-y}P$-based LDs operate at wavelengths longer than 600 nm, this leaves an uncharted green–yellow spectral gap that is directly relevant for emerging technologies such as the use of plastic optical fibers that require green lasers to achieve the lowest attenuation coefficient. Together with improvements in the degradation stability, this revives interest in $Zn_xCd_{1-x}Se$-based lasers that can cover this part of the spectrum [2]. A large effort has been devoted to the development of emitters with a quantum dot (QD) active layer and QD-based LDs have been demonstrated [3]. However, their performance is limited to well below room temperature by the thermal escape of excitons from confined states towards non-radiative recombination channels [4].

In this letter, we report the observation of efficient free exciton (FE) luminescence at room temperature in strongly confining $Zn_{0.5}Cd_{0.5}Se/Mg_xZn_yCd_{1-x-y}Se$ quantum wells (QWs). We demonstrate that the confinement of excitons in deep and narrow QWs ($d_{QW}\sim3$ nm or 10 ml) both stabilizes FEs and prevents their escape to the barriers, resulting in efficient radiative recombination at room temperature. Further, the high quality of these lattice-matched structures reduces the influence of non-radiative centers. Both these factors counteract the usual mechanisms that quench luminescence with increasing temperature, leading to FE emission at room temperature with an intensity that is ~40% of the emission intensity at low temperatures.

QW structures are grown by molecular beam epitaxy

* Corresponding author. Tel.: +1-814-863-9514; fax: +1-814-865-3604.
E-mail address: maksimov@netzero.net (O. Maksimov).

0038-1098/$ - see front matter © 2004 Elsevier Ltd. All rights reserved.
doi:10.1016/j.ssc.2004.07.022

(MBE) on (001) InP substrates, as described elsewhere [5]. They consist of a lattice matched $In_{0.5}Ga_{0.5}As$ buffer layer, $Mg_xZn_yCd_{1-x-y}Se$ barrier layers ($x\sim0.5$, $E_g\approx3.0$ eV), and a $Zn_{0.5}Cd_{0.5}Se$ ($E_g\approx2.18$ eV) well layer. The thickness of the bottom and the top barriers are 500 and 100 nm, respectively. QWs are characterized by photoluminescence (PL) and electroreflectance spectroscopies. PL measurements are performed in a liquid He continuous flow cryostat in a temperature range from 10 to 300 K. The 404-nm line of a LD is used for the excitation. The PL is collected in a backscattering geometry, spectrally resolved by a monochromator and detected by a cooled charge coupled device array detector. Electroreflectance measurements are performed at room temperature as described elsewhere [6].

Fig. 1 shows the PL spectrum at 10 K of a structure with a 3 nm wide well. (The 10 K PL spectra of structures with slightly different well widths are shown in the inset.) The barrier emission is at 2.978 eV and the QW emission is at 2.312 eV. The QW emission is significantly stronger than the barrier emission, suggesting that the majority of photoexcited carriers are captured by the QW prior to recombination. The absence of deep level emission is indicative of high crystalline quality. Since most of the band discontinuity in the $Mg_xZn_yCd_{1-x-y}Se/Zn_{0.5}Cd_{0.5}Se$ system is in the conduction band ($\Delta E_C/\Delta E_g\sim0.8$) [6], the conduction and valence band offsets are 533 and 133 meV, respectively. This is larger than for $Zn_xCd_{1-x}Se/ZnS_ySe_{1-y}$ QWs [7,8] and significantly exceeds the thermal activation energy providing sufficient quantum confinement even at room temperature ($k_BT=25$ meV).

Fig. 2 shows PL spectra of a 3 nm thick QW taken at different temperatures. The 10 K PL spectrum is dominated by a single spectral peak (A) that has an asymmetric line shape with a low energy tail. A higher energy peak B ($\Delta E=$ 22 meV) emerges at $\sim$30 K. As the temperature increases, both peaks red shift and the intensity of A decreases, while that of B increases. Finally, A disappears above 100 K while B persists up to room temperature and exhibits a gradual red shift, accompanied by a decrease in intensity and an increase in linewidth.

Fig. 3 shows room temperature electroreflectance (dotted line) and PL (solid line) spectra for comparison. The energy of the PL emission corresponds to the electron-heavy hole excitonic transition suggesting the free excitonic (FE) origin of luminescence. Based upon its position and temperature dependence, the higher energy peak (B) is assigned to a FE. The lower energy peak (A) can be attributed to a bound exciton (BE), biexciton, or charged exciton. To identify its origin, we study the dependence of the peak emission intensity on the excitation laser density at 10, 60, 100 and 300 K. Superlinear behavior is not observed indicating the

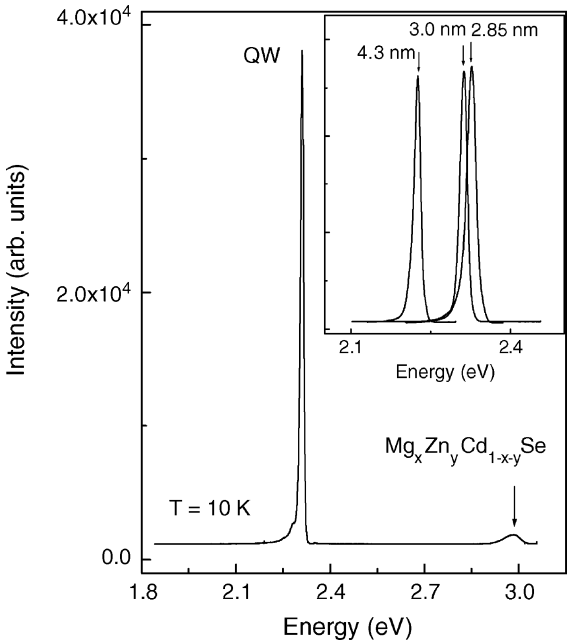

Fig. 1. Photoluminescence (PL) spectrum of a $Zn_{0.5}Cd_{0.5}Se/Mg_xZn_yCd_{1-x-y}Se$ quantum well (QW) structure with a 3 nm thick well layer taken at 10 K. The inset of the figure shows 10 K PL spectra of QW structures with different well thickness.

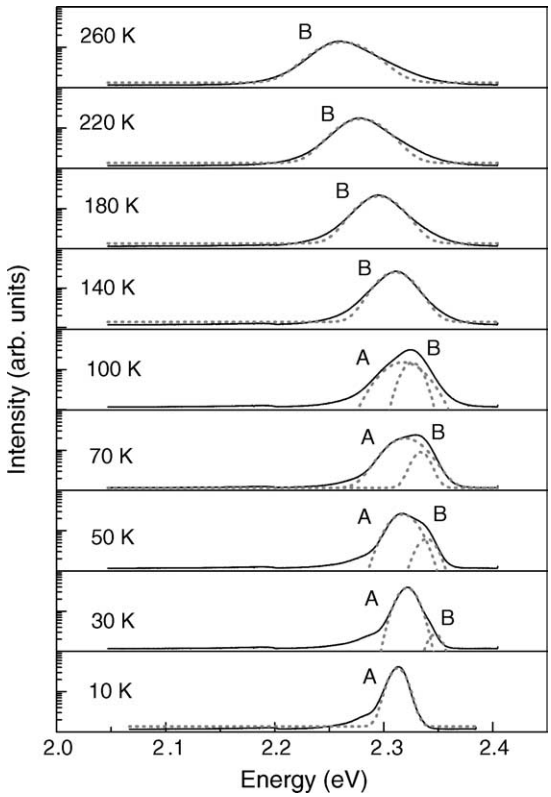

Fig. 2. Photoluminescence spectra of a 3 nm thick $Zn_{0.5}Cd_{0.5}Se/Mg_xZn_yCd_{1-x-y}Se$ QW taken at different temperatures. The solid lines correspond to the spectra while the dotted lines are Gaussian fits.

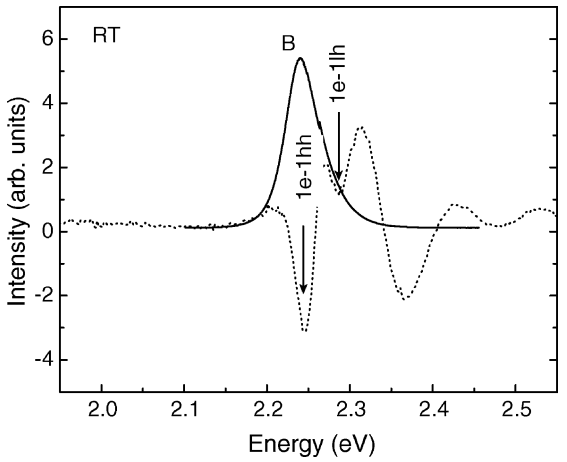

Fig. 3. Room temperature photoluminescence (solid line) and electroreflectance (dotted line) spectra of a 3 nm thick $Zn_{0.5}Cd_{0.5}Se/Mg_xZn_yCd_{1-x-y}Se$ QW.

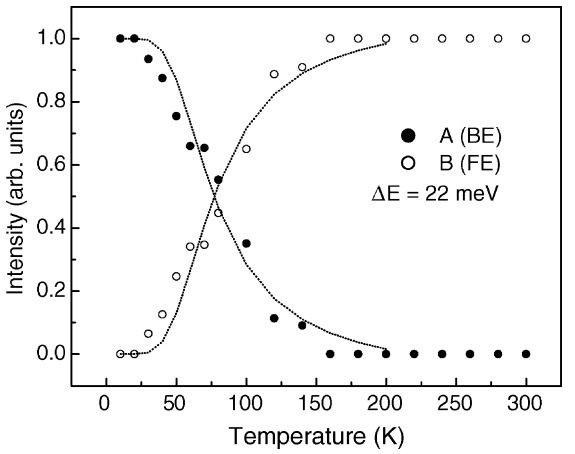

Fig. 4. Dependence of the integrated intensity of bound exciton (solid circles) and free exciton (open circles) emission lines as a function of temperature for a 3 nm thick $Zn_{0.5}Cd_{0.5}Se/Mg_xZn_yCd_{1-x-y}Se$ QW. The dotted lines are the fits.

absence of biexcitons or charged excitons. Instead, we find that the intensity of both peaks A and B increases linearly with excitation laser density and a slope (k) near unity is obtained over the whole temperature range (Table 1). This shows the excitonic origin of the emission [9] that persists up to room temperature.

To elucidate whether a BE contributes to the QW luminescence, we plot the integrated PL intensity for A and B as a function of temperature in Fig. 4. For convenience and to avoid the use of absolute intensities (A), the integrated intensity (I) is defined as:

$$I_J(T) = A_J(T)/(A_A(T) + A_B(T)) \quad J = A, B \tag{1}$$

The emission intensity is proportional to both the population density of excitons (N_j) and recombination efficiency (n_j):

$$A_J = n_j N_j \tag{2}$$

The n_j is expressed as a function of radiative (τ_R) and non-radiative (τ_{NR}) recombination times [10]:

$$n_j = (1 + \tau_R/\tau_{NR})^{-1} \tag{3}$$

Since BEs are thermally activated to FEs, the N_j can be described as $\sim[1-\exp(-\Delta E/k_BT)]$ for BEs and $\sim[0+\exp(-\Delta E/k_BT)]$ for FEs, where ΔE is the energy binding exciton to localization center. If we assume that recombination efficiency does not change with temperature and neglect other level depopulation mechanisms, we can write the integrated intensity of BE and FE lines as:

$$I_{BE} = n_{BE}\,(1 - \exp(-\Delta E/k_BT)/[n_{BE}(1 - \exp(-\Delta E/k_BT) + n_{FE}\exp(-\Delta E/k_BT)] \tag{4}$$

$$I_{FE} = n_{FE}\exp(-\Delta E/k_BT)/[n_{BE}(1 - \exp(-\Delta E/k_BT) + n_{FE}\exp(-\Delta E/k_BT)] \tag{5}$$

The fit based on this simplified model is shown with dotted lines in Fig. 4. It follows the experimental data and justifies the assignment of B to FE emission and A to BE emission. The recombination efficiency for FEs, estimated from the fit, is higher than the BE recombination efficiency ($n_{FE}/n_{BE} = 7.7$). This is in agreement with the observation that FEs have a shorter radiative recombination time than BEs [11]. The gap between BE and FE lines (ΔE) decreases with increasing QW thickness, from 24 meV for a 2.85 nm thick well to 20 meV for a 4.3 nm thick well, as shown in Table 1. The origin of the BE emission is unclear and can be explained by different mechanisms. First, since the well thickness is smaller than the exciton Bohr radius ($a_0 \sim 4.9$ nm) [12], while the confinement potential is

Table 1
Properties of the $Zn_{0.5}Cd_{0.5}Se/Mg_xZn_yCd_{1-x-y}Se$ quantum well structures

d_{QW} (nm)	k at 10 K	k at 60 K	k at 300 K	PL Intensity at 10 K (arb. units)	PL Intensity at 100 K (arb. units)	PL Intensity at 300 K (arb. units)	ΔE (meV)	E_B^0 (Cl^0X) (meV)	E^{2D} (meV)
2.85	1.05	1.08	1.18	1	1.30	0.95	24	22.0	42.9
3	1.06	1.11	1.18	1	0.78	0.23	22	21.7	42.2
4.3	1.05	1.06	1.22	1	1.02	0.4	20	19.0	37.0

large, roughness of the well/barrier interface and/or alloy disorder in the barrier layers can provide significantly deep localization states. Second, composition fluctuations in $Zn_{0.5}Cd_{0.5}Se$ alloy forming the well can cause exciton localization in the regions with increased cadmium content [13,14]. However, since $Zn_{0.5}Cd_{0.5}Se/Mg_xZn_yCd_{1-x-y}Se$ QWs are lattice matched in contrast to compressively strained $Zn_xCd_{1-x}Se/ZnSe$ QWs, the formation of cadmium-rich regions is unlikely. Finally, donor and/or acceptor bound excitons can contribute to the emission. $ZnCl_2$ cell is installed in MBE system and routinely used for *n*-type doping. Thus, due to the background doping, recombination of neutral donor bound excitons (Cl^0X) is likely to contribute at low temperatures. The Cl^0X binding energy (E_B^0) is ~9 meV in ZnSe [15]. Quantum confinement will increase (E_B^0) to 20–22 meV, as shown in Table 1. The estimated values are close to ΔE, indicating that Cl^0X recombination is a possible origin of the BE line.

The intensity of the QW emission is shown as an Arrhenius plot in Fig. 5. All QWs exhibit strong room temperature luminescence, comparable to that at 10 K. They also exhibit a non-monotonic dependence of the intensity on temperature. This temperature dependence is anomalous for $Zn_xCd_{1-x}Se$ QWs [7,8,16], but can be explained by a BE to FE transition. At low temperatures, where the BE emission dominates the decrease in emission intensity with increasing temperature is caused by thermal excitation of BEs to FEs. Over the temperature range 75–125 K, the increase in emission intensity is due to the higher FE recombination

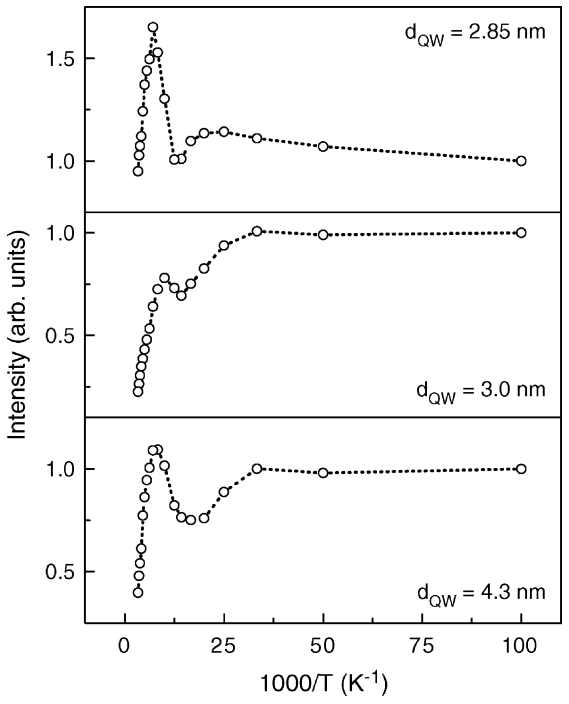

Fig. 5. Arrhenius plot of the emission intensity versus inverse temperature.

efficiency. At the highest temperatures studied, the decrease in intensity is caused by exciton dissociation, exciton escape from the well to the barriers, and/or the transfer to the non-radiative recombination centers. However, the decrease is small and the room temperature emission intensity is still ~40% of that at 100 K, as shown in Table 1. We believe this is due to the suppression of the mechanisms mentioned above.

We now estimate the increase in exciton binding energy due to the QW confinement using the results of a proven analytical technique [17]. For an infinitely deep QW, the exciton binding energy (E^{2D}) can be written as:

$$E^{2D} = E^{3D}/\{[1 + (\alpha - 3)/2]\}^2, \tag{6}$$

where E^{3D} is the exciton binding energy in the bulk, and α is a dimensionless parameter that varies with the quantum well width d_{QW} as follows:

$$\alpha = 3 - \exp(-d_{QW}/2a_0). \tag{7}$$

For a finite confinement potential, where wave function decay into the barrier decreases confinement, the above results are modified by defining an effective length scale d_{QW}^* [14] as:

$$d_{QW}^* = (2/j_B) + d_{QW} \tag{8}$$

where $1/j_B = 1/j_{BE} + 1/j_{BH}$, j_{BE} and j_{BH} are the wave vector solutions of the transcendental equations that result from solving the relevant Schrödinger equations for electrons and holes in the QW potential. The results of our calculations (Table 1) show that the exciton binding energy increases from the bulk value of 17.5 meV [18] to ~40 meV, preventing exciton dissociation even at room temperature.

We next use a semi-empirical model to estimate the carrier loss due to the thermally activated escape from the well (η) [16]:

$$\eta = 1 - 2/(2 + 100T \exp(-E/k_B T)) \tag{9}$$

where T is the temperature and E is the confinement energy. A 350 meV confinement limits carrier loss to 1% at room temperature. In our case confinement energy exceeds 650 meV and thermal escape is negligible.

Finally, we address the issue of transfer to non-radiative recombination centers, which is well known to significantly decrease room temperature luminescence. For instance, in material systems such as $In_xGa_{1-x}N$ with large misfit dislocation densities, this mechanism results in a rapid drop of emission intensity in $In_xGa_{1-x}N$ QWs ($T > 150$ K) [19] and degrades room temperature performance of $In_xGa_{1-x}N$ LEDs (defect density ~10^9 cm^{-2}) [20]. Since $Mg_xZn_yCd_{1-x-y}Se$ heterostructures are lattice matched and the defect density is small ($< 10^5$ cm^{-2}) [5], we do not expect this mechanism to be efficient.

In conclusion, $Zn_{0.5}Cd_{0.5}Se/Mg_xZn_yCd_{1-x-y}Se$ QWs are characterized by PL spectroscopy. BE emission dominates below 50 K, while FE emission dominates

above 100 K and persists up to room temperature. The room temperature emission is strong and comparable to the low temperature emission due to the efficient quantum confinement that suppresses non-radiative recombination mechanisms. This indicates high quantum efficiency and suggests that $Zn_{0.5}Cd_{0.5}Se/Mg_xZn_yCd_{1-x-y}Se$ QWs are attractive for application as lasers, operating in green spectral range. Finally, we note that these excitonic light emitters may also play an important role in the development of triggered single photon sources that function at elevated temperatures [21].

Acknowledgements

M.M., H.L., and M.C.T. were supported by NSF through grant ECS0217646. O.M. and N.S. acknowledge the support of the DARPA-QUIST program through the Center for Spintronics and Quantum Computation, University of California-Santa Barbara.

References

[1] S. Nakamura, M. Senoh, S. Nagahama, N. Matsushita, T. Mukai, Appl. Phys. Lett. 76 (2000) 22.
[2] S.V. Ivanov, Phys. Status Solidi A 192 (2002) 157.
[3] S.V. Ivanov, A.A. Toropov, S.V. Sorokin, T.V. Shubina, V. Sedova, A.A. Sitnikova, P.S. Kop'ev, Zh.I. Alferov, A.A. Waag, H.J. Lugauer, G. Reuscher, M. Keim, G. Landwehr, Appl. Phys. Lett. 74 (1999) 498.
[4] I.C. Robin, R. Andre, L.S. Dang, H. Mariette, S. Tatarenko, J.M. Gerard, K. Kheng, F. Tinjod, M. Bartels, K. Lischka, D. Schikora, Phys. Status Solidi B 241 (2004) 543.
[5] L. Zeng, S.P. Guo, Y.Y. Luo, W. Lin, M.C. Tamargo, H. Xing, S.G. Cargill III, J. Vac. Sci. Technol. B 17 (1999) 1255.
[6] M. Muñoz, H. Lu, X. Zhou, M.C. Tamargo, F.H. Pollak, Appl. Phys. Lett. 83 (2003) 1995.
[7] E. Oh, S.D. Lee, H.D. Jung, J.R. Kim, M.D. Kim, B.J. Kim, J.K. Li, H.S. Park, T.I. Kim, S.V. Ivanov, A.A. Toropov, T.V. Shubina, J. Appl. Phys. 80 (1996) 5951.
[8] I. Lo, K.H. Lee, L.W. Tu, J.K. Tsai, W.C. Mitchel, R.C. Tu, Y.K. Su, Solid State Commun. 120 (2001) 155.
[9] T. Schmidt, K. Lischka, W. Zulehner, Phys. Rev. B 42 (1992) 8989.
[10] M. Sugarawa, Phys. Rev. B 51 (1995) 10743.
[11] L. Aigouy, V. Mathet, F. Liaci, B. Gil, O. Briot, T. Cloitre, M. Averous, L. Aloumbard, Phys. Rev. B 53 (1996) 4708.
[12] I. Hernandez-Calderon, in: M.C. Tamargo (Ed.), II–VI Semiconductor Materials and Their Applications, Taylor and Franics, New York, 2002.
[13] S. Permogorov, A. Klochikhin, A. Reznitsky, J. Lumin. 100 (2002) 243.
[14] S. Permogorov, A. Klochikhin, A. Reznitsky, L. Tenishev, S. Ivanov, S. Sorokin, C. Klingshirn, J. Cryst. Growth 214 (2000) 1158.
[15] S.Z. Wang, S.F. Yoon, L. He, X.C. Shen, J. Appl. Phys. 90 (2001) 2314.
[16] C. Morhain, G.D. Brownlie, E. Tournie, A. Masi, C. Ongaretto, K.A. Prior, J.P. Faurie, B.C. Cavenett, J. Cryst. Growth 184 (1998) 591.
[17] H. Mathieu, P. Lefebrve, P. Christol, J. Appl. Phys. 72 (1992) 300.
[18] J. Camacho, I. Loa, A. Cantarero, I. Hernandez-Calderon, Microelectron. J. 33 (2002) 349.
[19] N. Grandjean, B. Damilano, J. Massies, S. Dalmasso, Solid State Commun. 113 (2000) 495.
[20] T. Stephan, M. Kunzer, P. Schlotter, W. Pletschen, H. Obloh, S. Müller, K. Köhler, J. Wagner, Phys. Status Solidi A 194 (2002) 568.
[21] K. Sebald, P. Michler, T. Passow, D. Hommel, G. Bacher, A. Forchel, Appl. Phys. Lett. 81 (2002) 2920.